Supporting Information
on

Graphene Oxide Coatings on Amino Acid-Modified Fe Surfaces for Corrosion Inhibition

Ankit Yadav, Rajeev Kumar and Balaram Sahoo*

Materials Research Centre, Indian Institute of Science, Bangalore, India-560012

**Corresponding author's email: bsahoo@iisc.ac.in*

S1. Characterization

The surface morphology of the CI, GO, GO/PABA-CI, GO/Gly-CI and GO/Ala-CI composites was demonstrated by Scanning Electron Microscope (SEM). X-Ray Diffraction (XRD) patterns were recorded using a PANalytical X-ray diffractometer (operated at 40 kV and 150 mA) in a 2θ range of 5° to 90° (Cu-K_α radiation, λ = 1.540 Å). Raman spectra of graphene oxide, PABA-CI, Gly-CI, Ala-CI, GO/PABA-CI, GO/Gly-CI and GO/Ala-CI samples were taken using a LabRam HR equipment (532 nm laser source).

S2. Color photograph of grafted samples

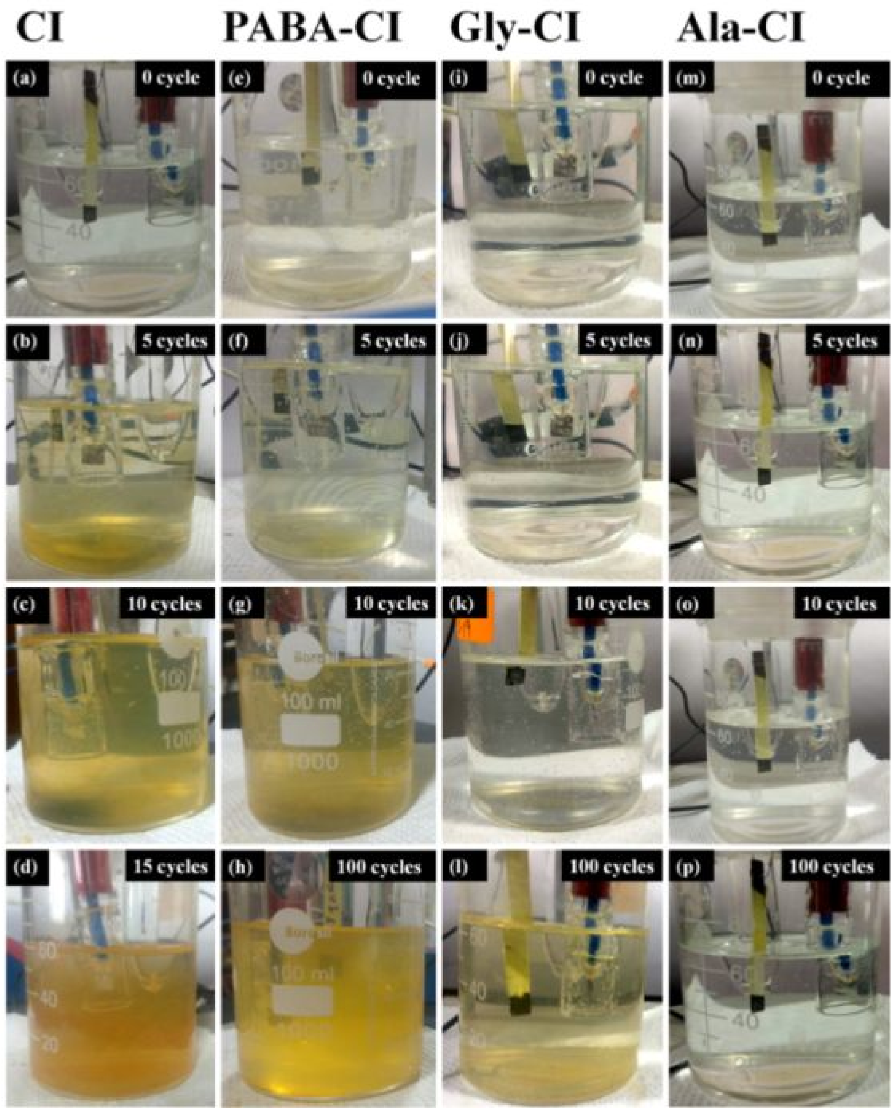

Fig.S1. Photos of the pure and grafted CI particles, presenting the change in color of the electrolytic-solution. (a) before and after (b) 5^{th}, (c) 10^{th} and (d) 15^{th} cycle of CV measurements for the CI-sample; (e) before and after (f) 5^{th}, (g) 10^{th} and (h) 100^{th} cycle for PABA-CI-sample; (i) before and after (j) 5^{th}, (k) 10^{th} and (l) 100^{th} cycle for Gly-CI-sample; and (m) before reaction, after (n) 5 cycles, (o)10 cycles and (p) 100 cycles of CV experiments for the electrode with Ala-CI-sample. We observe the change in color in case of CI, PABA-CI and Gly-CI.

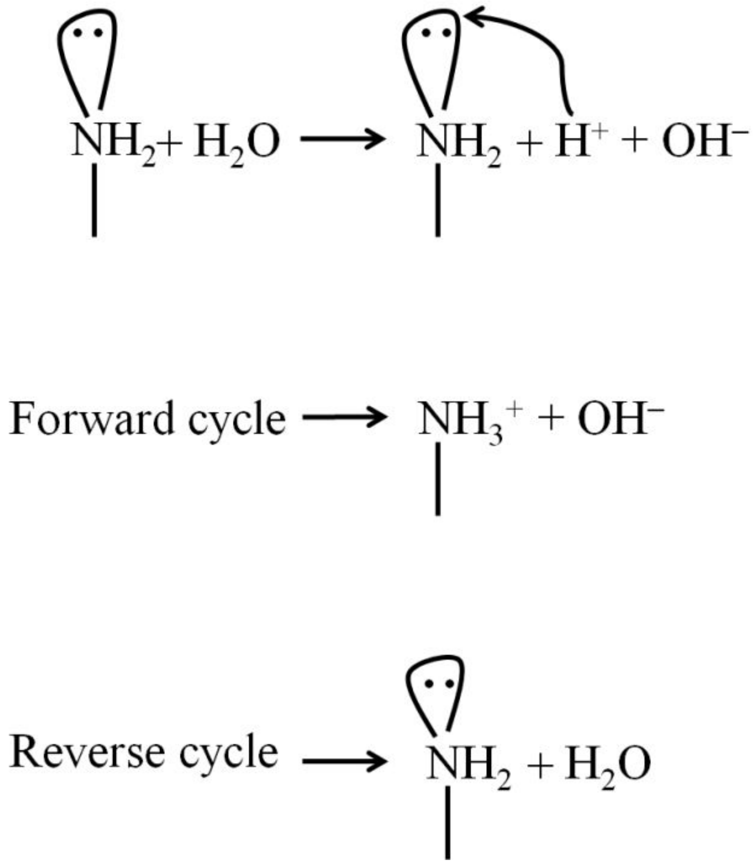

Fig.S2. Reaction process with the amino group of the grafted amino acids in aqueous solution.

Table S1. Kinetic parameters obtained from the Tafel analysis of CI, PABA-CI, Gly-CI and Ala-CI electrodes in 3M KCl aq. solution.

Sample	E_{corr} *(mV vs Ag/AgCl)*	i_{corr} *(μA/cm²)*	β_c *(mV/dec)*	β_a *(mV/dec)*	Corrosion rate (mm/yr)
CI	-593.15	270.04	364.2	294.5	12.53
PABA-CI					
(after 1st cycle)	26.41	18.58	259.9	216.0	
(after 100th cycle)	-478.36	161.21	347.6	285.7	7.49
Gly-CI					
(after 1st cycle)	117.62	19.98	124.0	161.7	
(after 100th cycle)	37.68	65.74	171.1	194.7	3.05
Ala-CI					
(after 1st cycle)	194.33	3.27	101.1	140.6	
(after 100th cycle)	161.35	4.07	124.2	181.2	0.189

S3. The corrosion rate formula [1]

From Faraday's first law which states:

"The amount of substance (w) liberated at electrode is directly proportional to the quantity of electricity (Q) passed".

$$W \propto Q \qquad\qquad Q = I \times t$$

$$W = Z \times I \times t \qquad\qquad Z = \frac{atomic\ mass\ (M)}{n \times 96500}$$

$$W = \frac{M \times I \times t}{n \times F} \quad (1) \qquad\qquad F = 96500\ C/mole$$

Dividing equation through t and surface area A, yields the corrosion rate (CR):

$$CR = \frac{M \times i}{n \times F} \quad (2)$$

Where, i (current density in $\mu A/cm^2$) = I/A

Current density rather than current is proportional to corrosion rate because the same current concentrated into smaller surface area results in a larger corrosion rate, corrosion rate is inversely proportional to area for same dissolving current.

Units of penetration per unit time result from dividing equation (2) by the density D of metal, for corrosion rate in mils per year (mpy) equation (2) becomes

$$CR = 0.129\,\frac{M \times i}{n \times D} \quad \text{(unit in mpy)} \quad (3)$$

1 mpy = 0.0254 mmpy

$$\Rightarrow CR = 0.00327\,\frac{M \times i}{n \times D}\ \text{(mm/yr)}$$

Hence, for Fe, $CR = \frac{Icorr \times K \times \text{Equivalent wieght}}{Area \times D}$, where K = 0.00327 mm/yr.

Table S2. Corrosion protection performances of graphene (Gr) based anticorrosive coatings [2-26]. The ratio of corrosion rates of graphene-based composite coated substrates ($CR_{uncoated}$) and that of uncoated substrates (CR_{coated}): $CR_{uncoated}/CR_{coated}$, is provided.

Metal Substrate	Electrolyte	Coating System	Immersion time	Ratio of corrosion rate ($CR_{uncoated}/CR_{coated}$)	Ref #
Steel	0.6 M NaCl	Silane/Gr composites	few hours	2000	2
Fe	0.6 M NaCl	Polymer/Gr composites	24 hours	15	3
Cu	0.1 M Na_2SO_4	CVD Gr + ALD Al_2O_3	3 hours	100	4
Ni	0.1 M NaCl	Thermal annealing grown Gr	few hours	7	5
Ni-Fe alloy	0.6 M NaCl	Laser irradiation grown Gr	1 hour	9	6
Cu	0.1 M NaCl	CVD Gr	few hours	10	7
Cu	0.6 M NaCl	Electrochemically deposited Gr	1 hour	18	8
Steel	0.6 M NaCl	Electrochemically deposited Ni/Gr	5 mins	2	9
Steel	0.6 M NaCl	Polymer/Gr composites	30 min	219	10
Steel	0.6 M NaCl	Nanocasted epoxy/ Gr composites	few hours	70	11
Steel	0.6 M NaCl	Polymer/Gr composites	30 min	200	12
Cu	0.6 M NaCl	Polymer/Gr composites	100 hours	140	13
Steel	0.6 M NaCl	Electrochemically deposited Gr	30 mins	2	14
Zn	0.6 M NaCl	Electrochemically deposited Gr	1 hour	130	15
Fe	0.6 M NaCl	Polymer/Gr composites	24 hours	100	16
Steel	0.6 M NaCl	Epoxy/Gr composites	96 hours	120	17
Cu	0.1 M Na_2SO_4	CVD Gr	few hours	7	18
Al	0.5 M NaCl	Dip coated Gr	30 mins	1200	19
Cu	0.1 M NaCl	CVD Gr	1 hour	50	20
Steel	0.6 M NaCl	Ceramic/Gr composites	24 hours	500	21

Steel	0.08M NaCl	Polymer/Gr composites	1 hour	35	22
Al alloy	0.6 M NaCl	Silane/Gr composites	30 mins	580	23
Al alloy	0.6 M NaCl	Silane/Gr composites	2 hours	10	24
Steel	0.6 M NaCl	Chitosan/Gr composites	6 hours	20	25
Mg alloy	0.6 M NaCl	Silane/Gr composites	80 mins	80	26
Fe particle	3 M KCl (extremely harsh condition)	Glycine/Gr composites	12 hours (accelerated current flow by CV)	76	This work

S4. Fitted Tafel plot for bare CI, PABA/Glycine/Alanine-CI samples and GO-coated-PABA-,Glycine-, Alanine-grafted-CI samples

We have obtained the best fits of the Tafel plots with the help of the software provided with the electrochemical instrument Biologic SP-200. The software is inbuilt for Tafel analysis as well as corrosion study. In the figure given in supporting information (Fig. S3-S15), the blue colored curve shows original and red colored curve show the fitted data for CI, PABA-CI, Gly-CI, Ala-CI, GO/PABA-CI, GO/Gly-CI and GO/Ala-CI sample.

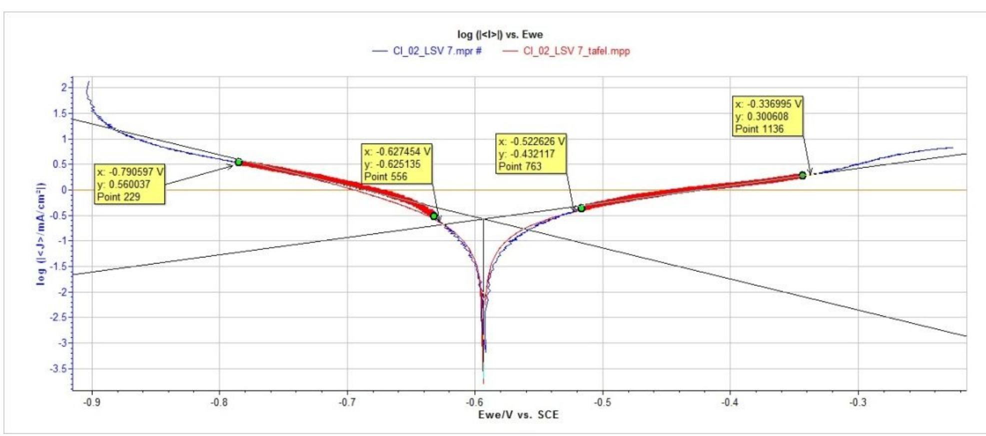

Fig.S3 Fitted Tafel plot for bare CI sample.

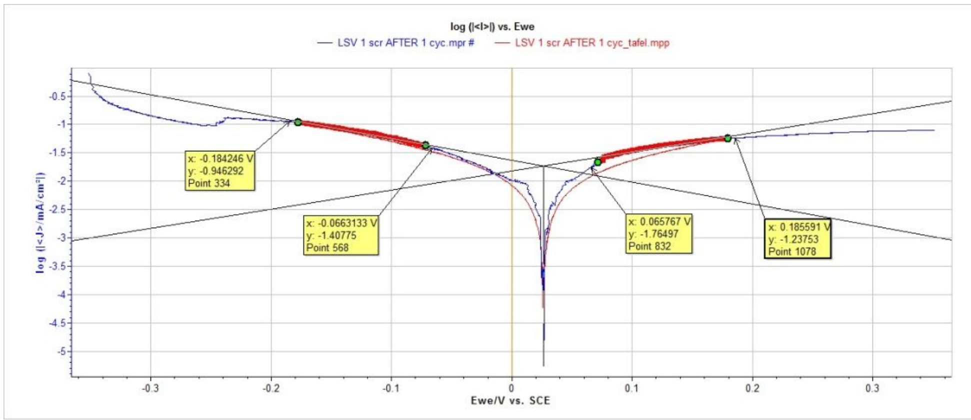

Fig.S4 Fitted Tafel plot for initial cycle of PABA-CI sample.

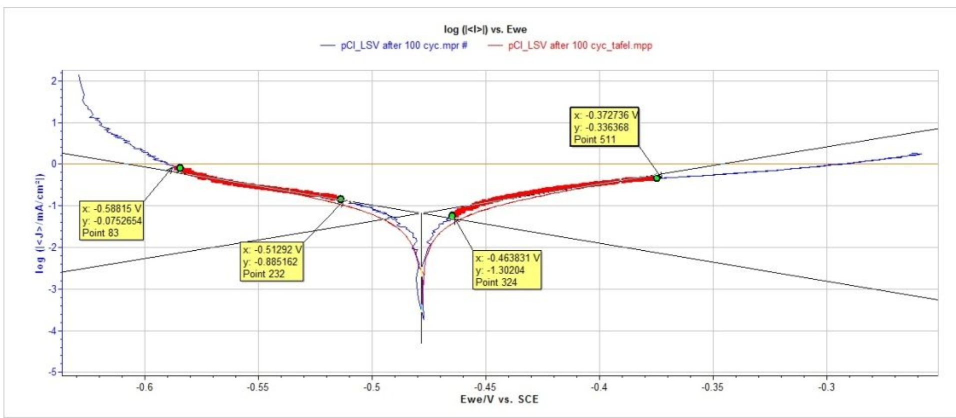

Fig.S5 Fitted Tafel plot for PABA-CI sample after 100 CV cycles.

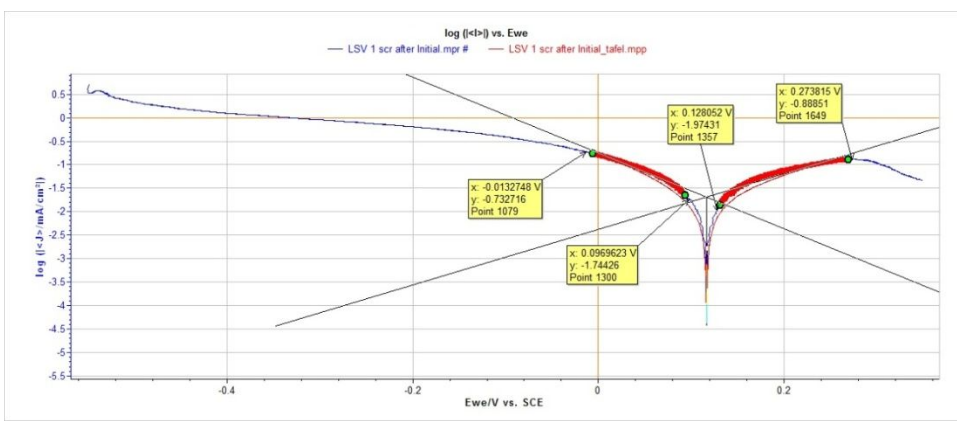

Fig.S6 Fitted Tafel plot for initial cycle of Gly-CI sample.

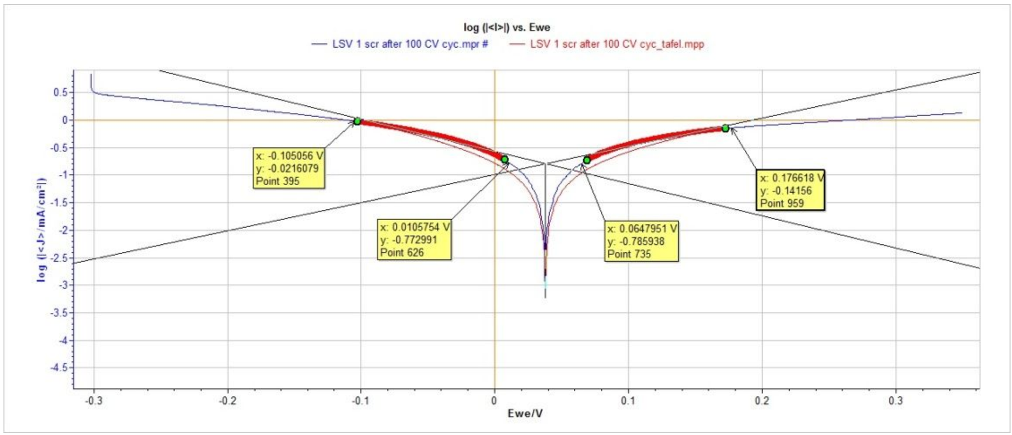

Fig.S7 Fitted Tafel plot for Gly-CI sample after 100 CV cycles.

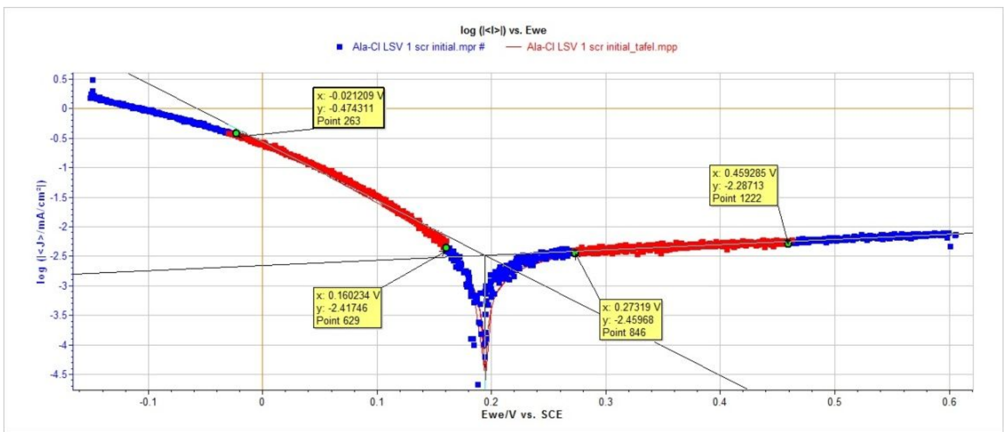

Fig.S8 Fitted Tafel plot for initial cycle of Ala-CI sample.

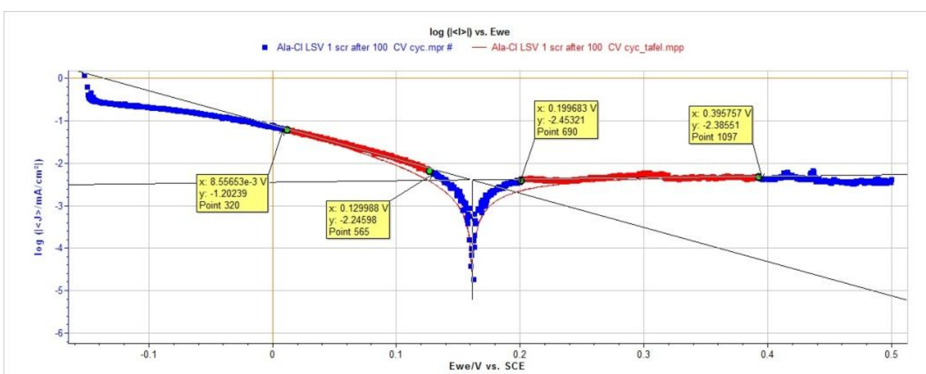

Fig.S9 Fitted Tafel plot for Ala-CI sample after 100 CV cycles.

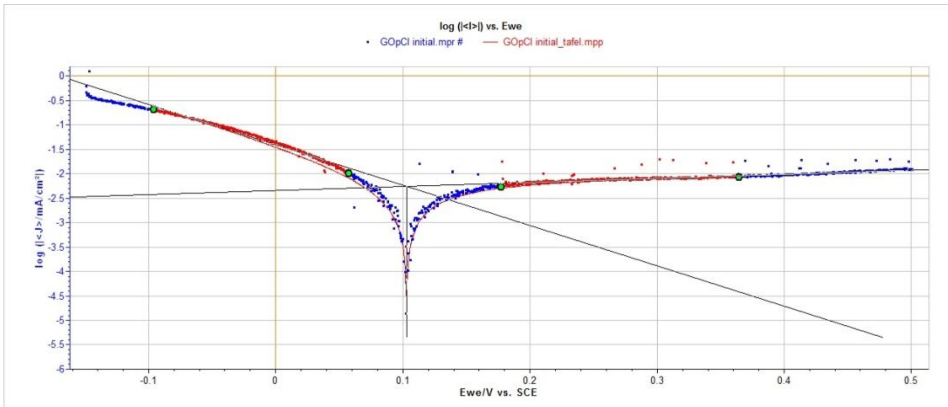

Fig.S10 Fitted Tafel plot for initial cycle of GO/PABA-CI sample.

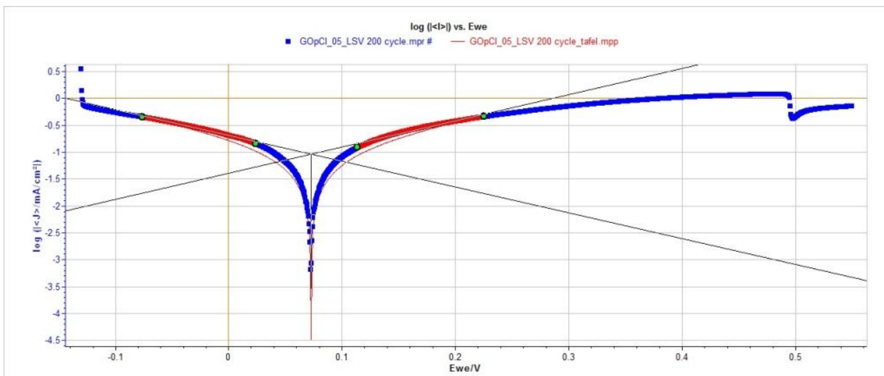

Fig.S11 Fitted Tafel plot for GO/PABA-CI sample after 200 CV cycles.

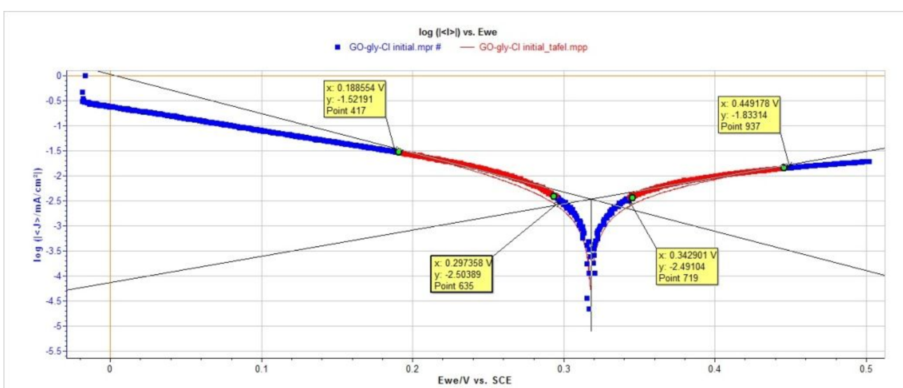

Fig.S12 Fitted Tafel plot for initial cycle of GO/Gly-CI sample.

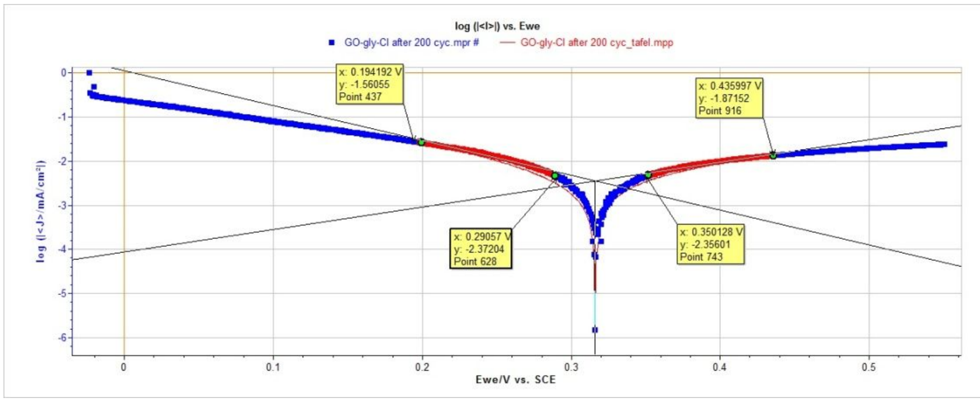

Fig.S13 Fitted Tafel plot for GO/Gly-CI sample after 200 CV cycles.

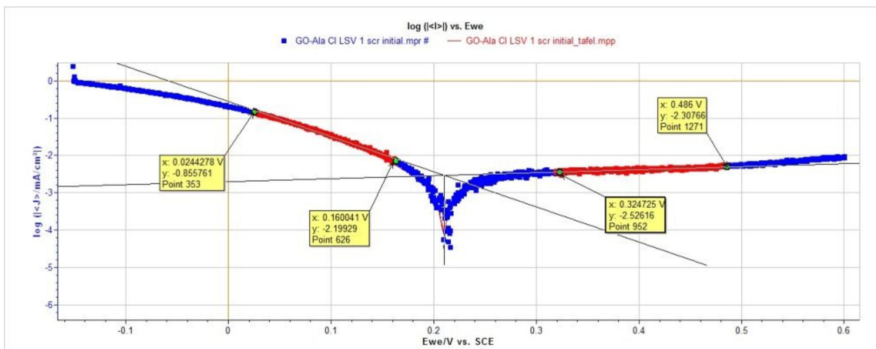

Fig.S14 Fitted Tafel plot for initial cycle of GO/Ala-CI sample.

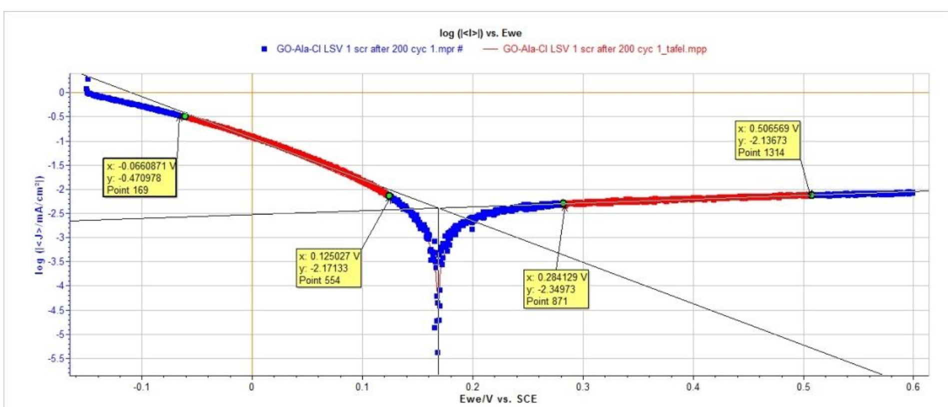

Fig.S15 Fitted Tafel plot for GO/Ala-CI sample after 200 CV cycles.

S5. Nyquist plots for CI and GO/PABA/Gly/Ala-CI samples (zoomed in separate images)

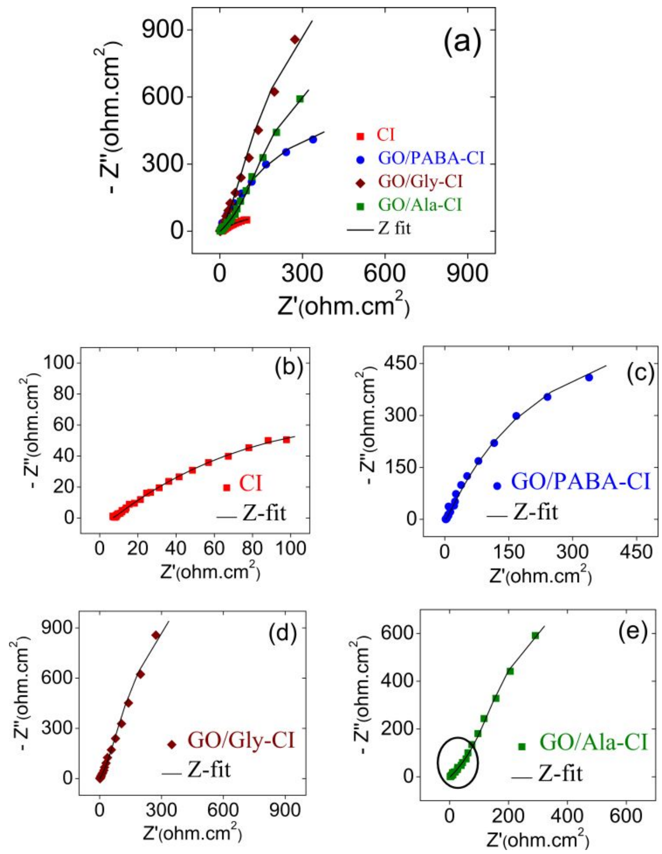

Fig.S16. (a) The combined Nyquist plots obtained from the impedance measurements in 3M KCl solution. For clarity individual Nyquist plots for bare CI (b) and GO/PABA-CI (c), GO/Gly-CI (d) and GO/Ala-CI (e), samples are also shown.

References

(1) Jones, D. A. *Principles and Prevention of Corrosion*, 2nd ed.; Prentice Hall: Upper Saddle River, NJ 07458, 1991.

(2) Aneja, K. S.; Bohm, S.; Khanna, A. S.; Bohm, H. L. M. Graphene Based Anticorrosive Coatings for Cr(VI) Replacement. *Nanoscale* **2015**, *7* (42), 17879–17888. https://doi.org/10.1039/c5nr04702a.

(3) Mo, M.; Zhao, W.; Chen, Z.; Liu, E.; Xue, Q. Corrosion Inhibition of Functional Graphene Reinforced Polyurethane Nanocomposite Coatings with Regular Textures. *RSC Advances* **2016**, *6* (10), 7780–7790. https://doi.org/10.1039/c5ra24823j.

(4) Hsieh, Y. P.; Hofmann, M.; Chang, K. W.; Jhu, J. G.; Li, Y. Y.; Chen, K. Y.; Yang, C. C.; Chang, W. S.; Chen, L. C. Complete Corrosion Inhibition through Graphene Defect Passivation. *ACS Nano* **2014**, *8* (1), 443–448. https://doi.org/10.1021/nn404756q.

(5) Mogera, U.; Kurra, N.; Radhakrishnan, D.; Narayana, C.; Kulkarni, G. U. Low Cost, Rapid Synthesis of Graphene on Ni: An Efficient Barrier for Corrosion and Thermal Oxidation. *Carbon* **2014**, *78* (Cvd), 384–391. https://doi.org/10.1016/j.carbon.2014.07.015.

(6) Ye, X.; Lin, Z.; Zhang, H.; Zhu, H.; Liu, Z.; Zhong, M. Protecting Carbon Steel from Corrosion by Laser in Situ Grown Graphene Films. *Carbon* **2015**, *94*, 326–334. https://doi.org/10.1016/j.carbon.2015.06.080.

(7) Shen, L.; Zhao, Y.; Wang, Y.; Song, R.; Yao, Q.; Chen, S.; Chai, Y. A Long-Term Corrosion Barrier with an Insulating Boron Nitride Monolayer. *Journal of Materials Chemistry A* **2016**, *4* (14), 5044–5050. https://doi.org/10.1039/c6ta01604a.

(8) Sahu, S. C.; Samantara, A. K.; Seth, M.; Parwaiz, S.; Singh, B. P.; Rath, P. C.; Jena, B. K. A Facile Electrochemical Approach for Development of Highly Corrosion Protective Coatings Using Graphene Nanosheets. *Electrochemistry Communications* **2013**, *32*, 22–26. https://doi.org/10.1016/j.elecom.2013.03.032.

(9) Kumar, C. M. P.; Venkatesha, T. V.; Shabadi, R. Preparation and Corrosion Behavior of Ni and Ni-Graphene Composite Coatings. *Materials Research Bulletin* **2013**, *48* (4), 1477–1483. https://doi.org/10.1016/j.materresbull.2012.12.064.

(10) Yu, Y. H.; Lin, Y. Y.; Lin, C. H.; Chan, C. C.; Huang, Y. C. High-Performance Polystyrene/Graphene-Based Nanocomposites with Excellent Anti-Corrosion Properties.

Polymer Chemistry **2014**, *5* (2), 535–550. https://doi.org/10.1039/c3py00825h.

(11) Chang, K. C.; Hsu, M. H.; Lu, H. I.; Lai, M. C.; Liu, P. J.; Hsu, C. H.; Ji, W. F.; Chuang, T. L.; Wei, Y.; Yeh, J. M.; et al. Room-Temperature Cured Hydrophobic Epoxy/Graphene Composites as Corrosion Inhibitor for Cold-Rolled Steel. *Carbon* **2014**, *66*, 144–153. https://doi.org/10.1016/j.carbon.2013.08.052.

(12) Chang, K. C.; Ji, W. F.; Lai, M. C.; Hsiao, Y. R.; Hsu, C. H.; Chuang, T. L.; Wei, Y.; Yeh, J. M.; Liu, W. R. Synergistic Effects of Hydrophobicity and Gas Barrier Properties on the Anticorrosion Property of PMMA Nanocomposite Coatings Embedded with Graphene Nanosheets. *Polymer Chemistry* **2014**, *5* (3), 1049–1056. https://doi.org/10.1039/c3py01178j.

(13) Qi, K.; Sun, Y.; Duan, H.; Guo, X. A Corrosion-Protective Coating Based on a Solution-Processable Polymer-Grafted Graphene Oxide Nanocomposite. *Corrosion Science* **2015**, *98*, 500–506. https://doi.org/10.1016/j.corsci.2015.05.056.

(14) Bagherzadeh, M.; Ghahfarokhi, Z. S.; Yazdi, E. G. Electrochemical and Surface Evaluation of the Anti-Corrosion Properties of Reduced Graphene Oxide. *RSC Advances* **2016**, *6* (26), 22007–22015. https://doi.org/10.1039/c5ra26948b.

(15) Li, R.; Liang, J.; Hou, Y.; Chu, Q. Enhanced Corrosion Performance of Zn Coating by Incorporating Graphene Oxide Electrodeposited from Deep Eutectic Solvent. *RSC Advances* **2015**, *5* (75), 60698–60707. https://doi.org/10.1039/c5ra11577a.

(16) Mo, M.; Zhao, W.; Chen, Z.; Yu, Q.; Zeng, Z.; Wu, X.; Xue, Q. Excellent Tribological and Anti-Corrosion Performance of Polyurethane Composite Coatings Reinforced with Functionalized Graphene and Graphene Oxide Nanosheets. *RSC Advances* **2015**, *5* (70), 56486–56497. https://doi.org/10.1039/c5ra10494g.

(17) Gu, L.; Liu, S.; Zhao, H.; Yu, H. Facile Preparation of Water-Dispersible Graphene Sheets Stabilized by Carboxylated Oligoanilines and Their Anticorrosion Coatings. *ACS Applied Materials and Interfaces* **2015**, *7* (32), 17641–17648. https://doi.org/10.1021/acsami.5b05531.

(18) Prasai, D.; Tuberquia, J. C.; Harl, R. R.; Jennings, G. K.; Bolotin, K. I. Graphene: Corrosion-Inhibiting Coating. *ACS Nano* **2012**, *6* (2), 1102–1108. https://doi.org/10.1021/nn203507y.

(19) Liu, J.; Hua, L.; Li, S.; Yu, M. Graphene Dip Coatings: An Effective Anticorrosion

Barrier on Aluminum. *Applied Surface Science* **2015**, *327* (37), 241–245. https://doi.org/10.1016/j.apsusc.2014.11.187.

(20) Raman, R. K. S.; Banerjee, P. C.; Lobo, D. E.; Gullapalli, H.; Sumandasa, M.; Kumar, A.; Choudhary, L.; Tkacz, R. Protecting Copper from Electrochemical Degradation by Graphene Coating. *Carbon* **2012**, *50* (11), 4040–4045. https://doi.org/10.1016/j.carbon.2012.04.048.

(21) Mondal, J.; Marques, A.; Aarik, L.; Kozlova, J.; Simões, A.; Sammelselg, V. Development of a Thin Ceramic-Graphene Nanolaminate Coating for Corrosion Protection of Stainless Steel. *Corrosion Science* **2016**, *105*, 161–169. https://doi.org/10.1016/j.corsci.2016.01.013.

(22) Jafari, Y.; Ghoreishi, S. M.; Shabani-Nooshabadi, M. Electrochemical Deposition and Characterization of Polyaniline-Graphene Nanocomposite Films and Its Corrosion Protection Properties. *Journal of Polymer Research* **2016**, *23* (5). https://doi.org/10.1007/s10965-016-0983-8.

(23) Zhu, H.; Yue, L.; Zhuang, C.; Zhang, Y.; Liu, X.; Yin, Y.; Chen, S. Fabrication and Characterization of Self-Assembled Graphene Oxide/Silane Coatings for Corrosion Resistance. *Surface and Coatings Technology* **2016**, *304*, 76–84. https://doi.org/10.1016/j.surfcoat.2016.07.002.

(24) Ahmadi, A.; Ramezanzadeh, B.; Mahdavian, M. Hybrid Silane Coating Reinforced with Silanized Graphene Oxide Nanosheets with Improved Corrosion Protective Performance. *RSC Advances* **2016**, *6* (59), 54102–54112. https://doi.org/10.1039/c6ra04843a.

(25) Fayyad, E. M.; Sadasivuni, K. K.; Ponnamma, D.; Al-Maadeed, M. A. A. Oleic Acid-Grafted Chitosan/Graphene Oxide Composite Coating for Corrosion Protection of Carbon Steel. *Carbohydrate Polymers* **2016**, *151*, 871–878. https://doi.org/10.1016/j.carbpol.2016.06.001.

(26) Ikhe, A. B.; Kale, A. B.; Jeong, J.; Reece, M. J.; Choi, S. H.; Pyo, M. Perfluorinated Polysiloxane Hybridized with Graphene Oxide for Corrosion Inhibition of AZ31 Magnesium Alloy. *Corrosion Science* **2016**, *109*, 238–245. https://doi.org/10.1016/j.corsci.2016.04.010.